Network Topology Impact on the Identification of Dynamic Network Models with Application to Autonomous Vehicle Platooning ⋆

Guilherme A. Pimentel * **Rafael de Vasconcelos** *
Aurélio Salton ** **Alexandre Bazanella** **

* *GACS - Group of Automation and Control Systems, Pontifícia Universidade Católica do Rio Grande do Sul, Brazil*
guilherme.pimentel@pucrs.br, vasconcelosrv@gmail.com
** *DELAE - Department of Automation and Energy, Universidade Federal do Rio Grande do Sul, Brazil*
<aurelio.salton,bazanella>@ufrgs.br

Abstract: The interconnection of complex devices in network structures has been a challenging topic in the system identification research domain. This study presents the model identification of autonomous vehicles in platoon formation, which can be cast as a dynamic network. The paper presents the comparison between two network structures: (i) a vehicle-based network, which considers the interconnection between the vehicles based only on the velocity measurements, and (ii) a sensor-based network that considers the available sensor, i.e. the velocity and the relative distance measurements. The comparison is based on the difference between the identified transfer functions and the true ones, and the analysis of the identified air resistance coefficient variances. In addition, the paper presents the identifiability requirements for both network topologies. Simulation results show that for the same data set the variance of the identified parameters can be almost five times smaller if the system is represented as a sensor-based network, but some conditions to guarantee the identifiability of this network structure must be fulfilled.

Keywords: Identification, dynamic network model, identifiability, network topologies, interconnected systems, autonomous vehicles

1. INTRODUCTION

In this paper, we study the parameter identification of autonomous vehicles in platoon formation, which can be represented as distributed control system. The concept of vehicle platooning is to form a convoy of vehicles driving close behind each other to increase the freeways traffic throughput and also reduce fuel consumption for the follower vehicles, transportation costs and greenhouse gas emissions (Liang et al., 2016). The study of platooning of autonomous vehicles has gain more attention as the traffic flow is increasing as the world economy grows, especially in freeways, due to the expansion of the freight transport (Liang et al., 2016). The road freight is responsible for the transportation of 49.0 % in Europe Union (EU Commission, 2018), 45.9 % in the USA (Wilmsmeier and Spengler, 2015) and 61.1 % in Brazil (CNT, 2019) of all goods. To achieve higher fuel efficiency, with economies up to 20% of fuel consumption (Liang et al., 2016), small spacing between two vehicles is required, which increases the risk of accident. One solution for this issue is the formation of autonomous vehicle platoons, which may maintain a desired spacing policy. Many studies can be found in the literature where controllers are designed with this objective (Dai et al., 2018; Liang et al., 2016; Sedran, 2016). However, most of these studies consider that the dynamic behavior of all vehicles in the platoon is the same, i.e. the same mathematical model is considered. Note that the vehicles masses or brake performances can vary, due to the load and unload of goods or depreciation of the breaking systems, which may cause accidents in autonomous vehicle if these changes are not considered when the platoon enter in a upper- or downhill road. Considering the fuel consumption, one of the main concerns is the air resistance forces in the vehicle aerodynamic, which changes considering the distances from the leader, weight, velocity and type of the vehicle (Alam et al., 2015; Sandberg, 2001). This parameter is extremely important to estimate the fuel consumption and to design reliable controllers.

The interconnection of a platoon can be represented as a dynamic network model, where one vehicle influences the dynamic behavior of the other, as a distributed control system. It is well know that complex network structure cannot be operated, designed, and maintained without the help of models (Dankers et al., 2016). The dynamic network modeling is defined as an interconnection of

⋆ This study was financed in part by the Coordenação de Aperfeiçoamento de Pessoal de Nível Superior - Brasil (CAPES) - Finance Code 001.

Copyright lies with the authors

transfer functions or modules where the interconnecting signals (terminals) are considered as nodes/vertices in the network, and proper transfer function are considered as links/edges (Goncalves and Warnick, 2008; Van den Hof et al., 2013; Gevers et al., 2018). In this paper, it is assumed that the interconnection structure (topology) of the network is known, and our goal is to identify the transfer functions in the network as in Van den Hof et al. (2013).

In this context, this study focuses on how to identify the transfer function of each vehicle in a platoon based on data from autonomous vehicle formation. Also, a comparison between two different network model representations of the dynamic system and its identified parameter variances are considered: (i) a vehicle-based network structure considering the velocity measurements and (ii) a sensor-based network structure considering velocity and the relative distance measurements.

2. MATHEMATICAL MODELING AND PROBLEM STATEMENT

This study considers a platooning formation of heavy-duty vehicles (HDVs). Figure 1 illustrates the platoon system architecture for an N vehicle platoon. The lead vehicle, with index $i = 1$, is to the left and the last vehicle is to the right. The control architecture for vehicle speed control is shown in front of each vehicle. The information flow in the system is given by the arrows (Alam et al., 2015).

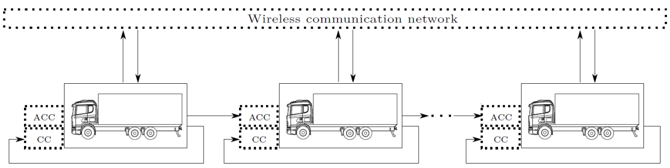

Fig. 1. Platoon system architecture for an N vehicle platoon. Adapted from Liang et al. (2016).

Each HDV has two layers of controllers and a connection to the wireless network to send relevant information between the vehicles. The bottom layer is the Cruise control (CC), where the controller acts in the speed of the vehicle considering the speed set by the driver. In the layer above the Advanced CC (ACC) uses a radar sensor to control the desired spacing to the preceding vehicles (Liang et al., 2016). Based on this structure, a suboptimal decentralized controller can be designed to maintain the vehicle formation, as presented in (Alam et al., 2015). In this paper we consider that when the gain of the controllers for each HDV are known, which is normally the case, it is possible to identify the transfer function of each HDV. Therefore, the model of each HDV and the dynamic network models can be represented as follows.

2.1 HDVs Mathematical Modeling

The dynamic equation of center of mass of the HDVs can be described by

$$m_t\dot{v} = k_eT_e - k_bF_{brake} - k_dv^2 - k_{fr}cos\alpha - k_gsin\alpha, \quad (1)$$

where v is the vehicle velocity, $\dot{v}$ is its derivative (acceleration), m_t denotes the accelerated mass and $T_e \in R$ denotes the net engine torque. k_e, k_b, k_d, k_{fr}, and k_g denote the characteristic vehicle and environment coefficients for the brake, air resistance, road friction, and gravitation respectively. α is the terrain slope and F_{brake} is the action of the brakes. Further explanation about the parameters can be found in Alam et al. (2015).

The nonlinear model (1) can be linearized with respect to cruise velocity v_o, an engine torque $T_{e,o}$ which maintains the velocity, a fixed time gap between the vehicles $\tau_{s,o}$, and a constant slope α_o.

The linearized equation of the HDV can be represented as

$$\begin{cases} \dot{v}_1 = -\dfrac{2k_{d,1}v_o}{m_{t,1}}v_1 + k_{e,1}T_{e,1}, \text{ (leader)} \\ \dot{v}_i = -\dfrac{2\tilde{k}_{d,i}v_o}{m_{t,i}}v_i + \dfrac{k_{d,i}v_o^2}{m_{t,i}}d_{(i-1)i} + k_{e,i}T_{e,i} \text{ (followers)}, \end{cases}$$

where $\tilde{k}_{d,i} > 0$ is the coefficient related to the air resistance and vehicle velocity and $k_{d,i} > 0$ is the coefficient or the air resistance related to the distance between two vehicles. Typical values for k_d ranges from 0.5 to 1.1 (Sandberg, 2001), and $\tilde{k}_{d,i} = k_d(1 - \Phi(d)/100)$, where $\Phi = 41.29 - 0.414d$, $d = \tau_sv$ and $v = v_o$ (Alam et al., 2015).

Assumption 1. The mass $m_{t,i}$ and the cruise velocity v_o are known or can be measured.

Assumption 2. The coefficients $k_{e,i}$ that transforms the engine torque ($T_{e,i}$) into linear force is known.

The platoon dynamics can be represented in a compact form for N vehicles

$$\begin{cases} \dot{v}_1 = \Theta_1v_1 + k_{e,1}T_{e,1} \text{ (leader)}, \\ \dot{v}_i = \Theta_iv_i + \delta_id_{(i-1)i} + k_{e,i}T_{e,i} \text{ (followers)}, \end{cases}$$

where $i = 2, ...N$ is the number of HDVs in formation.

$$\Theta_1 = -\frac{2k_{d,1}v_o}{m_{t,1}}, \; \Theta_i = -\frac{2\tilde{k}_{d,i}v_o}{m_{t,i}} \text{ and } \delta_i = -\frac{k_{d,i}v_o^2}{m_{t,i}}. \quad (2)$$

Considering the HDVs velocity as $(v_1, v_2, ..., v_N)$ and relative distance between the HDVs $(d_{12}, d_{23}, ...d_{(N-1)N})$, to maintain the formation one can design a state-feedback controller with the following control law (Alam et al., 2011)

$$T_{e,1} = -K_1^3v_1 + r_{v1}, \quad (3)$$

$$T_{e,i} = -K_i^1v_{(i-1)} - K_i^2d_{(i-1)i} - K_i^3v_i + r_{vi}, \quad (4)$$

where $T_{e,i}$ is the input torque for the i^{th} vehicle, the $K_i^{1,2,3}$ are the feedback gains and r_{vi} are the preset reference velocity.

The implementation of this control law gives the following closed-loop representation

$$\begin{aligned} \dot{v}_1 &= (\Theta_1 - k_{e,1}K_1^3)v_1 + r_{v,1}, \text{ (leader)} \\ \dot{v}_i &= (\Theta_i + k_{e,i}K_i^3)v_i + (\delta_i + k_{e,i}K_i^2)d_{(i-1)i} \\ &\quad -k_{e,i}K_i^1v_{(i-1)} + r_{v,i}. \text{ (followers)} \end{aligned}$$

2.2 Problem Statement

The objective of this study is to identify the transfer function model of each HDV and also the parameters k_d and $\tilde{k}_d$, which are linked to the air resistance coefficient. For that, measurements from the vehicle velocity (v_i) and relative distance ($d_{(i-1)i}$) are gathered with sample time

t_s. To proceed the identification procedure we first obtain the discrete transfer function using the *Euler Backward* approximation for the velocity equations

$$V_i(q^{-1}) = -\frac{-K_i^1 k_{e,i} t_s}{(K_i^3 k_{e,i} t_s - \Theta_i t_s + 1 - q^{-1})} V_{(i-1)}(q^{-1}) + \frac{(\delta_i t_s - K_i^2 k_{e,i} ts)}{K_i^3 k_{e,i} t_s - \Theta_i t_s + 1 - q^{-1}} D_{(i-1)i}(q^{-1}), \quad (5)$$

and for the relative distance

$$D_{(i-1)i}(q^{-1}) = (V_i(q^{-1}) - V_{(i-1)}(q^{-1}) t_s)/(q^{-1} - 1), \quad (6)$$

where q^{-1} is the backward shift operator, i.e. $q^{-1}u(t) = u(t-1)$. Based on the discrete transfer function the problem is cast in the dynamic network model representation.

2.3 Dynamic network model representation

In order to represent the studied problem in the framework of the identification of dynamical networks (Dankers et al., 2016; Gevers et al., 2018), we consider two network structures: (i) where each L node is the velocity of N HDV and (ii) where each L node corresponds to a particular sensor, i.e. velocity and relative distance, where the node signals can be denoted as $\omega_1(t), \ldots, \omega_L(t)$. These node signals are related to each other and to external excitation signal r_j and with noise signals e_j by the following network equation, which we call **network model** and in which the matrix G^0 will be called the **network matrix**:

$$\begin{bmatrix} \omega_1 \\ \omega_2 \\ \vdots \\ \omega_3 \end{bmatrix} = \begin{bmatrix} 0 & G_{12} & \cdots & G_{1L} \\ G_{21} & 0 & \ddots & G_{2L} \\ \vdots & \ddots & \ddots & \vdots \\ G_{L1} & G_{L2} & \cdots & 0 \end{bmatrix} \begin{bmatrix} \omega_1 \\ \omega_2 \\ \vdots \\ \omega_L \end{bmatrix} + K^0(q) \begin{bmatrix} r_1 \\ r_2 \\ \vdots \\ r_L \end{bmatrix} . + H^0(q) \begin{bmatrix} e_1 \\ e_2 \\ \vdots \\ e_L \end{bmatrix},$$

or

$$\omega(t) = G^0(q)\omega(t) + K^0(q)r(t) + H^0(q)e(t), \quad (7)$$

with the following properties (Gevers et al., 2018):

- G_{jp} are proper but not necessarily strictly proper transfer functions. Some of them may be zero, indicating that there is no link from $\omega_p(t)$ to $\omega_j(t)$;
- there is a delay in every loop going from one $\omega_p(t)$ to itself;
- the network is well-posed so that $(I - G^0)^{-1}$ is proper and stable;
- all node signals $\omega_p(t)$, $p = 1, \ldots, L$ are measurable.
- K^0 reflects how the external excitation signals affect the node signals.
- $e \in \mathcal{R}^L$ is an unmeasured disturbance, referred to as the process noise with positive definite covariance matrix Σ. $H(q)$ is a $L \times L$ stable rational matrix.
- the external excitation signals r_j are assumed to be uncorrelated with all noise signals $e_j, j = 1, \cdots, L$.

3. DYNAMIC NETWORK IDENTIFICATION

Among different identification methods for closed-loop system, we selected one of the most general method called Instrumental Variable (IV) (Söderström and Stoica, 1983).

3.1 The Instrumental Variable Method

In the case of network identification, the interconnection of the modules could result in

$$\hat{\omega}_j(t|t-1, \theta) = \phi(t)^T \theta_o + \upsilon_j(t). \quad (8)$$

Here θ_o is called the true parameter vector, and assumes that $\upsilon_j(t)$ is a stationary stochastic process that is independent of the input signal(Söderström and Stoica, 1983). In this case the estimation is consistent if (and essentially only if)

$$E\left[\phi(t)\phi^T(t)\right] \text{ is nonsingular,} \quad (9)$$

$$E\left[\phi(t)\upsilon(t)\right] = 0, \quad (10)$$

where E denoted the expectation operator. In the studied case, $\upsilon(t)$ is correlated noise which violates the second condition, as the disturbance $\upsilon(t)$ is correlated with the delayed output variables present in $\phi(t)$. One way to overcome this issue is to use the Instrumental variables (IV), which is a generalization of the LS estimate and is expressed as

$$\hat{\theta}_M^{IV} = \left[\frac{1}{M}\sum_{t=1}^{M} z(t)\phi^T(t)\right]^{-1} \left[\frac{1}{M}\sum_{t=1}^{M} z(t)\omega_j(t)\right], \quad (11)$$

where $z(t)$ is a vector of instrumental variables. There are several techniques to select the IV, for example instrumental variable in four steps, IV recursive, etc (for more details (Söderström and Stoica, 1983)). In this work the choice of the instrumental is the input signal of the network, the variable r_1 (the velocity set point for the platoon leader) where

$$z(t) = [\; r_1(t) \;\; r_1(t-1) \;\; r_1(t-2) \;\; \cdots \;\; r_1(t-M) \;]. \quad (12)$$

Before proceeding to the parameter identification step, an important definition has to be stated, according to (Gevers et al., 2013):

Definition 1. (**Identifiability at θ_1**) Consider a model at a given parameter value θ_1. The model is *locally identifiable at θ_1* if there exists a $\delta > 0$ and a data set $\boldsymbol{z}(\cdot) \triangleq \{u(\cdot), x_0\}$ such that, for all $\theta \in \| \theta - \theta_1 \| \leq \delta$, the outputs of the model with these two different parameter values θ and θ_1, both driven by the same data set are identical (i.e. $\omega(t,\theta) = \omega(t,\theta_1) \forall t > 0$) only if $\theta = \theta_1$. The model is *globally identifiable at θ_1* if the same holds for all $\delta > 0$. The model is *structurally identifiable* if it is identifiable at all θ.

4. HDV DYNAMIC NETWORK REPRESENTATION AND PARAMETER IDENTIFICATION

In this section, we present the identification procedure involving a platoon of three HDVs.The identification procedure is evaluated comparing the true value parameters to the identified ones and its variances. In the simulation procedure, similar as proposed by Alam et al. (2015), first it is considered that the HDV platoon is moving with constant speed of 70 km/h (v_o=70 km/h), meaning that the distance between the vehicles are constant as previously set ($\tau_{s,o}$=1s). The disturbance in the network is added by the leader that is forced to accelerate through a step input from 70 km/h to 80 km/h and after 60 second resume the cruise speed to 70km/h. This results in a step excitation in the platoon, as shown in Figure 2. The radar sensor, which measures the relative distance between the two HDVs, are considered to have white noise with variance 0.1. It is important to highlight that different from the work proposed by Dai et al. (2018); Liang et al. (2016); Sedran (2016), each vehicle has differently dynamic behavior,

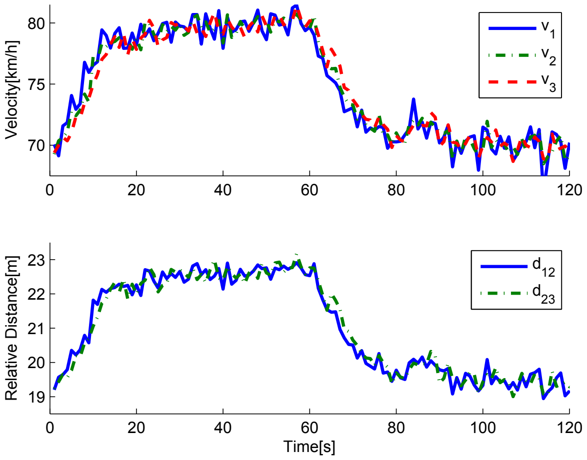

Fig. 2. Simulation data to identify HDVs transfer functions.

meaning that $m_{t,1} \neq m_{t,2} \neq m_{t,3}$, $\tilde{k}_{d,1} \neq \tilde{k}_{d,2} \neq \tilde{k}_{d,3}$ and $k_{d,1} \neq k_{d,2} \neq k_{d,3}$.

The simulation parameters are (Vehicle 1) $\tilde{k}_{d,1} = 0.6$, $k_{e,1} = 0.148 \times 10^{-3}$, $K_1^3 = 0.98 \times 10^3$, $m_{t,1} = 40000kg$; (Vehicle 2) $k_{e,2} = 0.148 \times 10^{-3}$, $K_2^1 = -6.56 \times 10^3$, $K_2^2 = -500.35 \times 10^3$, $K_2^3 = 590.03 \times 10^3$, $m_{t,2} = 30000kg$; (Vehicle 3) $k_{e,3} = 0.148 \times 10^{-3}$, $K_3^1 = -6.8 \times 10^3$, $K_3^2 = -590.35 \times 10^3$, $K_3^3 = 700.03 \times 10^3$, $m_{t,3} = 50000kg$ and $v_o = 19.44\ m/s$ $(70\ km/h)$.

4.1 Vehicle-Based Dynamic Network Representation for the Platoon Formation of HDVs

Assuming that the i^{th} vehicle controls the headway distance by using only information from the immediate preceding vehicle, the discrete transfer function from the lead vehicle's velocity $V_1(q^{-1})$ to the tail-end vehicle's velocity $V_N(q^{-1})$ can be expressed as

$$V_N(q^{-1}) = G_1^v(q^{-1})G_2^v(q^{-1}) \cdots G_{N-1}^v(q^{-1})V_1(q^{-1}), \quad (14)$$

where

$$V_i(q^{-1}) = G_i^v(q^{-1})V_{i-1}(q^{-1}), \quad i = 2, \ldots N. \quad (15)$$

where the superscript $(\cdot)^v$ means the vehicle-based dynamic network structure.

Figure 3 represents the block diagram of equation (14), which is represented as a branch network.

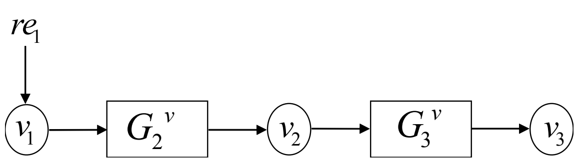

Fig. 3. Block diagram vehicle-based dynamic network

By combining (5) and (6) it is straight forward to derive the transfer function (15) where

$$G_i^v(q^{-1}, \hat{\theta}) = \frac{b_{0,i}^v + b_{1,i}^v q^{-1}}{a_{0,i}^v + a_{1,i}^v q^{-1} + a_{2,i}^v q^{-2}}, \quad (16)$$

with

$$a_{0,i}^v = (1 - (\Theta_i + k_{e,i}K_i^3)t_s + (\delta_i - k_{e,i}K_i^2)t_s^2), \quad (17)$$

$$a_{1,i}^v = ((\Theta_i + k_{e,i}K_i^3)t_s - 2), \quad (18)$$

$$a_{2,i}^v = 1, \quad (19)$$

$$b_{0,i}^v = (\delta_i - k_{e,i}K_i^2)t_s^2 + (-k_{e,i}K_i^1)t_s, \quad (20)$$

$$b_{1,i}^v = (k_{e,i}K_i^1)t_s. \quad (21)$$

Considering the IV method (11) and (16) we define

$$\hat{\theta}_i^v = \left[a_{0,i}^v \ a_{1,i}^v \ a_{2,i}^v \ b_{0,i}^v \ b_{1,i}^v\right], \quad (22)$$

$$\phi_2^v = \left[-v_2[k] \ -v_2[k-1] \ -v_2[k-2] \ v_1[k] \ v_1[k-1]\right], \quad (23)$$

$$\phi_3^v = \left[-v_2[k] \ -v_3[k-1] \ -v_3[k-2] \ v_2[k] \ v_2[k-1]\right], \quad (24)$$

where $i = \{2, 3\}$ and the instrumental variable as (12).

Simulations are carried out considering $n = 1000$ different realizations of the relative distance sensor noise, which is a white noise with variance 0.1. The network is identifiable as the network has the structure of a branch. Therefore, the IV method, presented in the section 3.1, uses the data to estimate the vehicles transfer function and also the air resistance coefficients. To obtain the desired parameters ($k_{d,i}$ and $\tilde{k}_{d,i}$) first we compute Θ_i and δ_i using equations (18) and (20), respectively, and after equations presented in (2). Figures 5(a) and 5(d), show the bode representation of the difference between true vehicle model and the identified one. Also, Table 1 presents the true values, the estimated mean values and its variances for the identification of the air resistance coefficients. In the following we present the results for the sensor-based network identification and later the comparison between both results.

4.2 Sensor-Based Dynamic Network Representation for the Platoon Formation of HDVs

The network matrix G^0 from equation (7) represents the interconnection of the HDVs. Taking the closed-loop discrete equations of the platoon formation, equations (5) and (6), and the measurements from velocity sensor and relative distance sensor, the network matrix can be expressed as (13).

The identifiability of the dynamic network must be analyzed in order to obtain the correct identification of the network parameters. Considering that the only excitation signal is given by the leader of the platoon ($re_1(t) \neq 0$) and the parameters of the HDV no. 2 are desired, we must guarantee independent excitations to their in-neighbours, here we have $v_1(t)$, $v_2(t)$ and $d_{12}(t)$ are uncorrelated signals, otherwise the parameter subset is non-identifiable. In figure 4 we can see that the signal $v_1(t)$ is correlated with $v_2(t)$ and $d_{12}(t)$ when there is no noise in the measurements. This means that the network is not identifiable unless there is uncorrelated noise in the measurements of velocity and relative distance, i.e. $re_2(t) \neq re_3(t) \neq 0$. For the HDV no. 3 we have a similar result, where we must guarantee the signals $v_2(t), v_3(t)$ and $d_{23}(t)$ are uncorrelated, to guarantee the network identifiability. Normally, in practice all measurements have noise and that is an advantage for the dynamic network identification.

$$\begin{bmatrix} v_1(t) \\ d_{12}(t) \\ v_2(t) \\ d_{23}(t) \\ v_3(t) \end{bmatrix} = \begin{bmatrix} 0 & 0 & 0 & 0 & 0 \\ \frac{t_s}{1-z^{-1}} & 0 & -\frac{t_s}{1-z^{-1}} & 0 & 0 \\ -\frac{k_{e,2}K_2^1 t_s}{(-\Theta_2 + k_{e,2}L_2^3)t_s + 1 - z^{-1}} & \frac{(\delta_2 - k_{e,2}K_2^2)t_s}{(-\Theta_2 + k_{e,2}K_2^3)t_s + 1 - z^{-1}} & 0 & 0 & 0 \\ 0 & 0 & \frac{t_s}{1-z^{-1}} & 0 & -\frac{t_s}{1-z^{-1}} \\ 0 & 0 & -\frac{k_{e,3}K_3^1 t_s}{(-\Theta_3 + k_{e,3}K_3^3)t_s + 1 - z^{-1}} & \frac{(\delta_3 - k_{e,3}K_3^2)t_s}{(-\Theta_3 + k_{e,3}K_3^3)t_s + 1 - z^{-1}} & 0 \end{bmatrix} \begin{bmatrix} v_1(t) \\ d_{12}(t) \\ v_2(t) \\ d_{23}(t) \\ v_3(t) \end{bmatrix} + \begin{bmatrix} re_1(t) \\ re_2(t) \\ re_3(t) \\ re_4(t) \\ re_5(t) \end{bmatrix}. \tag{13}$$

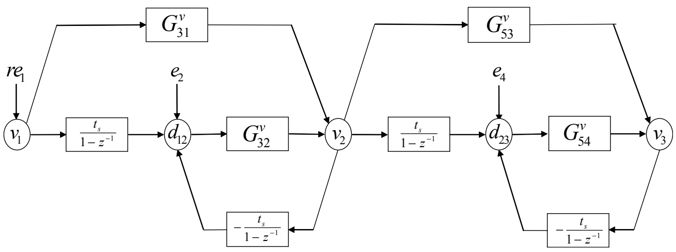

Fig. 4. Block diagram sensor-based dynamic network represented by equation (13).

Base on the equation (13) the modules or the discrete transfer functions to be identified are presented by

$$G^s_{(j(j-2))}(q^{-1}, \hat{\theta}) = \frac{b^s_{0,i}}{a^s_{0,i} + a^s_{1,i}q^{-1}}, \tag{25}$$

$$G^s_{(j(j-1))}(q^{-1}, \hat{\theta}) = \frac{d^s_{0,i}}{c^s_{0,i} + c^s_{1,i}q^{-1}}, \tag{26}$$

with $j = \{3, 5\}$ and $i = \{2, 3\}$, where superscript $(\cdot)^s$ means the sensor-based dynamic network with

$$b^s_{0,i} = k_{e,i}K_i^1 t_s, \tag{27}$$

$$d^s_{0,i} = (\delta_i - k_{e,i}K_i^2)t_s, \tag{28}$$

$$a^s_{0,i} = c^s_{0,i} = (\Theta_i - k_{e,i}K_i^3)t_s + 1, \tag{29}$$

$$a^s_{1,i} = c^s_{1,i} = 1. \tag{30}$$

The parameters are identified using the IV method (11), (25) and (26). Based on that we define

$$\hat{\theta}^s_{(j(j-2))} = \left[a^s_{0,i} \; a^s_{1,i} \; b^s_{0,i}\right], \tag{31}$$

$$\phi^s_{(j(j-2))} = \left[-v_i[k] \; -v_i[k-1] \; v_{(i-1)}[k]\right], \tag{32}$$

$$\hat{\theta}^s_{(j(j-1))} = \left[c^s_{0,i} \; c^s_{1,i} \; d^s_{0,i}\right], \tag{33}$$

$$\phi^s_{(j(j-1))} = \left[-v_i[k] \; -v_i[k-1] \; d_{(i-1)i}[k]\right]. \tag{34}$$

and consider the instrumental variable as (12).

The identification procedure uses the same data set presented in the previous section. As the system is represented as a sensor-based dynamic network, which considers the measurements of $v_1(t), v_2(t)$ and $d_{12}(t)$, where $d_{12}(t)$ (the radar sensor of HDV no. 2) has noisy measurements for the identification of HDV no. 2. Similar regressor is considered for the third vehicle, but in this case it uses the measurements of $v_2(t), v_3(t)$ and $d_{23}(t)$, where $d_{23}(t)$ (the radar sensor of HDV no. 3) has noisy measurements for the identification of HDV no. 3. To obtain the desired parameters ($k_{d,i}$ and $\tilde{k}_{d,i}$) first we compute Θ_i and δ_i using equations (29) and (28), respectively, and after equations presented in (2). The true values, the estimated mean values and its variance are presented in Table 1.

Figure 5 presents the bode diagrams from the difference between the identified transfer functions and the true ones. The first line of plots is linked to the HDV no. 2 and the second line HDV no. 3. The first column are the vehicle-based identification results and the other two columns are the sensor-based identification results. Note that transfer functions from the sensor-based identification are more accurate than the vehicle-base identification with magnitudes around 10^{-9}. Comparing the results from Table 1 is evident that the variance of the estimated parameters for the sensor-based dynamic network representation are almost five times smaller then the vehicle-based structure, as presented in Figure 5(f). It is important to highlight that the data set from velocities used for both identification procedure are the same. This shows the impact of the dynamic network structure on the variance of the estimate. Depending on the network structure of the system we can obtain the same model with reduced order, which impacts in the variance of the estimates. In addition the results shows that the 'deeper' is the desired transfer function in the network, if the identifiability is guarantee, smaller in the variance in the identified models, resulting in a more reliable model for control purposes.

5. CONCLUSION

The identification of dynamic network model is useful for many applications in distributed control systems. In this paper we have presented an identification method to identify the transfer functions, and consequently, the air resistance coefficients for N number of HDVs in a platoon formation. Also, the identifiability of the network has been analyzed when the excitation is imposed by the leader of the platoon. Two different dynamic network representations were presented for the same system, (i) vehicle-based and (ii) sensor-based. In the latter, the difference between the identified transfer functions and the true ones, and the variances of the air resistance coefficients, become much smaller when compared with the former case. As future work we will give special attention to analyze the results of estimating all the modules simultaneously and also study the sufficient excitation conditions (persistence of excitation) for consistency of the parameters estimation.

REFERENCES

Alam, A., Møartensson, J., and H.Johansson, K. (2015). Experimental evaluation of decentralized cooperative cruise control for heavy-duty vehicle platooning. *Control Engineering Practice*, 38, 11–25.

Alam, A.A., Gattami, A., and Johansson, K.H. (2011). Suboptimal decentralized controller design for chain structures: Applications to vehicle formations. In *50th*

Table 1. Air resistance coefficient identification results $n = 1000$

Parameter	True Value	Estimated Values (Vehicle-Based Structure)		Estimated Values (Sensor-Based Structure)	
		Mean	Variance	Mean	Variance
$k_{d,2}$	1.100×10^0	1.097×10^0	1.230×10^{-2}	1.099×10^0	2.979×10^{-6}
$\tilde{k}_{d,2}$	8.228×10^{-1}	8.240×10^{-1}	2.729×10^{-3}	8.228×10^{-1}	6.567×10^{-7}
$k_{d,3}$	8.000×10^{-1}	8.009×10^{-1}	2.983×10^{-2}	8.000×10^{-1}	3.673×10^{-9}
$\tilde{k}_{d,3}$	5.340×10^{-1}	5.336×10^{-1}	6.704×10^{-3}	5.340×10^{-1}	8.209×10^{-10}

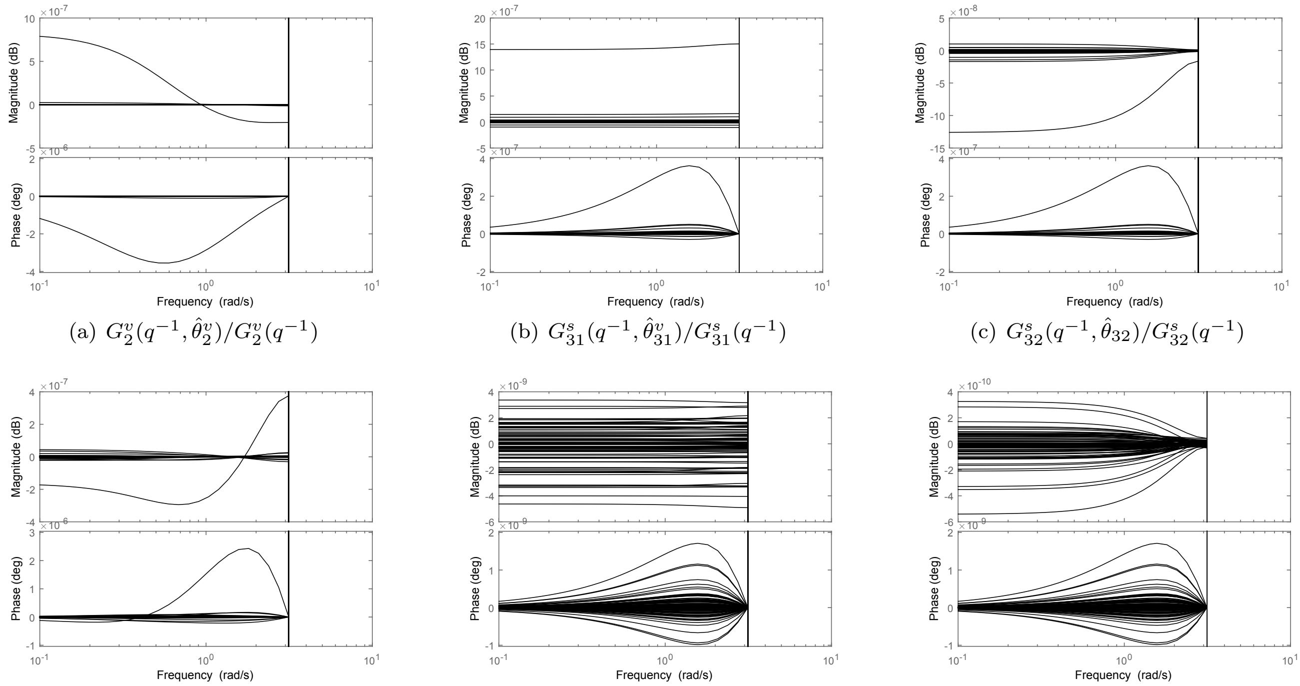

(a) $G_2^v(q^{-1}, \hat{\theta}_2^v)/G_2^v(q^{-1})$ (b) $G_{31}^s(q^{-1}, \hat{\theta}_{31}^v)/G_{31}^s(q^{-1})$ (c) $G_{32}^s(q^{-1}, \hat{\theta}_{32})/G_{32}^s(q^{-1})$

(d) $G_3^v(q^{-1}, \hat{\theta}_3^v)/G_3^v(q^{-1})$ (e) $G_{53}^s(q^{-1}, \hat{\theta}_{53})/G_{53}^s(q^{-1})$ (f) $G_{54}^s(q^{-1}, \hat{\theta}_{54})/G_{54}^s(q^{-1})$

Fig. 5. Bode Diagram from the difference between identified and true transfer function. The first row is linked to the HDV no. 2 and the second row HDV no. 3. The first column are the vehicle-based identification results and the other two columns are the sensor-based identification results.

IEEE Conference on Decision and Control and European Control Conference (CDC-ECC).

CNT (2019). Statistical report - Confederação Nacional do Transporte CNT - february 2019. Technical report.

Dai, S.L., He, S., Lin, H., and Wang, C. (2018). Platoon formation control with prescribed performance guarantees for usvs. *IEEE Transactions on Industrial Electronics*, 65.

Dankers, A., Van den Hof, P.M.J., Bombois, X., and Heuberger, P.S.C. (2016). Identification of dynamic models in complex networks with prediction error methods: Predictor input selection. *IEEE Transactions on Automatic Control*, 61(4), 937–952.

EU Commission (2018). EU Transport - Statistical Pocketbook 2018. Technical report, European Commission.

Gevers, M., Bazanella, A., Coutinho, D., and Dasgupt, S. (2013). Identifiability and excitation of linearly parametrized polynomial systems. In *Proceedings of 52nd IEEE Conference on Decision and Control (CDC2013)*, volume 1.

Gevers, M., Bazanella, A.S., and Pimentel, G.A. (2018). *Emerging Applications of Control and Systems*, chapter Identification of Dynamical Networks, 151 – 163. Springer International Publishing AG.

Goncalves, J. and Warnick, S. (2008). Necessary and sufficient conditions for dynamical structure reconstruction of LTI networks. *IEEE Transactions on Automatic Control*, 53 (7), 1670 – 1674.

Liang, K.Y., Martensson, J., and Johansson, K.H. (2016). Heavy-duty vehicle platoon formation for fuel efficiency. *IEEE Transactions on Intelligent Transportation Systems*, 17(4).

Sandberg, T. (2001). *Heavy Truck Modeling for Fuel Consumption Simulations and Measurements*. Ph.D. thesis, Linköping Studies in Science and Technology.

Sedran, S. (2016). *A truck dynamics model for driving simulators*. Ph.D. thesis, Automotive Engineering Department of Applied Mechanics Gothenburg.

Söderström, T. and Stoica, P. (1983). *Instrumental Variable Methods for System Identification*. Springer, Berlin, Heidelberg.

Van den Hof, P.M., Dankers, A., Heuberger, P.S., and Bombois, X. (2013). Identification of dynamic models in complex network with prediction error methods - basic methos for consistent module estimates. *Automatica*, 49, 2994 – 3006.

Wilmsmeier, G. and Spengler, T. (2015). The evolution of modal split in freight transport in south america, 2000-2013. *Cepal - Bulletin FAL*, 343(7).